NASA/TM—2018–220167

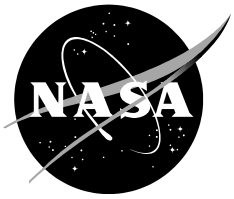

# TESS Data Release Notes:
## Sector 4, DR5

*Michael M. Fausnaugh, Christopher J. Burke*
*Kavli Institute for Astrophysics and Space Science, Massachusetts Institute of Technology, Cambridge, Massachusetts*

*Douglas A. Caldwell*
*SETI Institute, Mountain View, California*

*Jon M. Jenkins*
*Ames Research Center, Moffett Field, California*

*Jeffrey C. Smith, Joseph D. Twicken*
*SETI Institute, Mountain View, California*

*Roland Vanderspek*
*Kavli Institute for Astrophysics and Space Science, Massachusetts Institute of Technology, Cambridge, Massachusetts*

*John P. Doty*
*Noqsi Aerospace Ltd, Billerica, Massachusetts*

*Jie Li*
*SETI Institute, Mountain View, California*

*Eric B. Ting*
*Ames Research Center, Moffett Field, California*

*Joel S. Villasenor*
*Kavli Institute for Astrophysics and Space Science, Massachusetts Institute of Technology, Cambridge, Massachusetts*

**February 6, 2019**

## Acknowledgements

These Data Release Notes provide information on the processing and export of data from the Transiting Exoplanet Survey Satellite (TESS). The data products included in this data release are target pixel files, light curve files, collateral pixel files, full frame images (FFIs), cotrending basis vectors (CBVs), and Data Validation (DV) reports, time series, and associated xml files.

These data products were generated by the TESS Science Processing Operations Center (SPOC, Jenkins et al., 2016) at NASA Ames Research Center from data collected by the TESS instrument, which is managed by the TESS Payload Operations Center (POC) at Massachusetts Institute of Technology (MIT). The format and content of these data products are documented in the Science Data Product Description Document (SDPDD)[1]. The SPOC science algorithms are based heavily on those of the Kepler Mission science pipeline, and are described in the Kepler Data Processing Handbook (Jenkins, 2017).[2] The Data Validation algorithms are documented in Twicken et al. (2018) and Li et al. (2019). The TESS Instrument Handbook (Vanderspek et al., 2018) contains more information about the TESS instrument design, detector layout, data properties, and mission operations.

The TESS Mission is funded by NASA's Science Mission Directorate.

This report is available in electronic form at
https://archive.stsci.edu/tess/

[1] https://archive.stsci.edu/missions/tess/doc/EXP-TESS-ARC-ICD-TM-0014.pdf
[2] https://archive.stsci.edu/kepler/manuals/KSCI-19081-002-KDPH.pdf

# 1 Observations

TESS Sector 4 observations include physical orbits 15 and 16 of the spacecraft around the Earth. Two operational anomalies occurred during Sector 4—an incorrect guide star table and an instrument shutdown—and are discussed in §1.1. Data collection was paused for for 1.04 days during perigee passage while downloading data. In total, there are 22.23 days of science data collected in Sector 4.

Table 1: Sector 4 Observation times

| | UTC | TJD[a] | Cadence # |
|---|---|---|---|
| Orbit 15 start | 2018-10-19 09:34:28 | 1410.89974 | 132081 |
| Guidestar tables replaced | 2018-10-21 18:19:59 | 1413.26468 | 133783 |
| Instrument anomaly start | 2018-10-27 00:52:00 | 1418.53691 | 137579 |
| Data collection resumed | 2018-10-29 17:03:40 | 1421.21168 | 139505 |
| Orbit 15 end | 2018-11-01 00:11:40 | 1423.50890 | 141159 |
| Orbit 16 start | 2018-11-02 01:09:21 | 1424.54897 | 141908 |
| Orbit 16 end | 2018-11-14 08:21:39 | 1436.84918 | 150764 |

[a] TJD = TESS JD = JD - 2,457,000.0

The spacecraft was pointing at RA (J2000): 55.007°; Dec (J2000): −36.642°; Roll: 203.83°. Two-minute cadence data were collected for 20,000 targets, and full-frame images were collected every 30 minutes. See the TESS project Sector 4 observation page[3] for the coordinates of the spacecraft pointing and center field-of-view of each camera, as well as the detailed target list. Fields-of-view for each camera with all two-minute targets can be found at the TESS Guest Investigator Office observations status page[4].

## 1.1 Operations Anomalies

An incorrect guide star table was loaded into the DHU at the beginning of Sector 4. The impact on spacecraft stability was negligible, but the spacecraft pointing was offset by ∼4 arc-seconds from where it would have pointed had the correct guide star table been loaded. Thus, once the correct guide star table was loaded (TJD 1413.26), the spacecraft pointing shifted by ∼4 arc-seconds.

At TJD 1418.54, an interruption in communications between the instrument and spacecraft occurred, resulting in an instrument turn-off until TJD 1421.21. No data or telemetry were collected during this period.

## 1.2 Notes on Individual Targets

Three very bright stars (Tmag $\lesssim$ 2) with large pixel stamps were not processed in the photometric pipeline. Target pixel files with raw data are provided, but no light curves were produced. The affected TIC IDs are 328228602, 92252969, and 38877693.

[3] https://tess.mit.edu/observations/sector-4

[4] https://heasarc.gsfc.nasa.gov/docs/tess/status.html

One target (140072113) had a very bright star nearby (140072112). The contaminating flux for this object is very large and the pipeline assigns it a disjoint photometric aperture, which likely causes uncorrected systematic errors in the light curves.

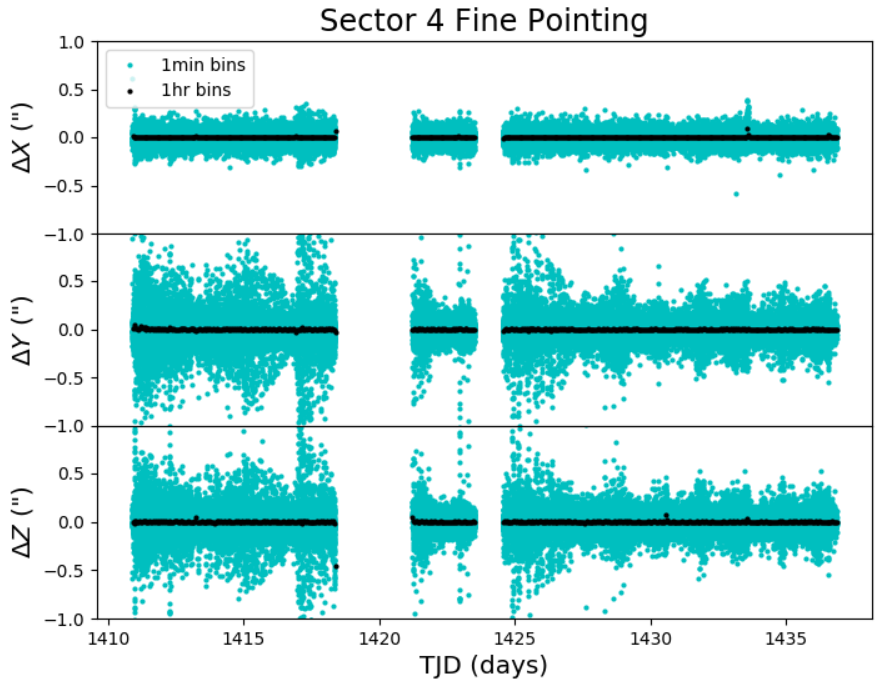


Figure 1: Guiding corrections based on spacecraft fine pointing telemetry. The delta-quaternions from each camera have been converted to spacecraft frame, binned to 1 minute and 1 hour, and averaged across cameras. Long-term trends (such as those caused by differential velocity aberration) have also been removed. The ΔX/ΔY directions represent offsets along the the detectors' rows/columns, while the ΔZ direction represents spacecraft roll. The gap in the first half of the sector is the instrument anomaly (see §1).

## 1.3 Spacecraft Pointing and Momentum dumps

Sector 4 was the first set of science observations with an improved Attitude Control System (ACS) algorithm. The new ACS mode displays significantly lower pointing jitter than the previous configuration—the RMS scatter of the guiding corrections are over an order of magnitude smaller than those for Sectors 1–3.

For the first ∼2.5 days of observations, an error in the uploaded guidestar tables resulted in a fractional pixel offset between the expected and commanded locations of Camera 1 and Camera 4. The ACS averages these offsets, resulting in a pointing close to the intended location; the true pointing was offset by about 4 arcseconds (∼0.2 pixels) from the commanded pointing. The guidestar tables were corrected at TJD 1413.26, removing the 4 arcsecond offset. The pointing offset and guidestar table errors did not have any effect on the pointing stability.

As in Sector 1, the reaction wheel speeds were reset to low values with momentum dumps every 2.5 days. FFIs taken during these times were marked with bit 6 (Reaction Wheel Desaturation Events). Only one or two FFIs are affected by each momentum dump.

Figure 1 summarizes the pointing performance over the course of the sector based on Fine Pointing telemetry. The ordinate axis is a factor of five smaller than in previous data releases ($-1$ to 1 arcsecond, rather than $-5$ to 5 arcseconds). The gap towards in the first half of the sector marks the instrument anomaly. The other periods of increased dispersion are generally correlated with the reaction wheels running at high speeds, and in some cases are correlated with the times of momentum dumps.

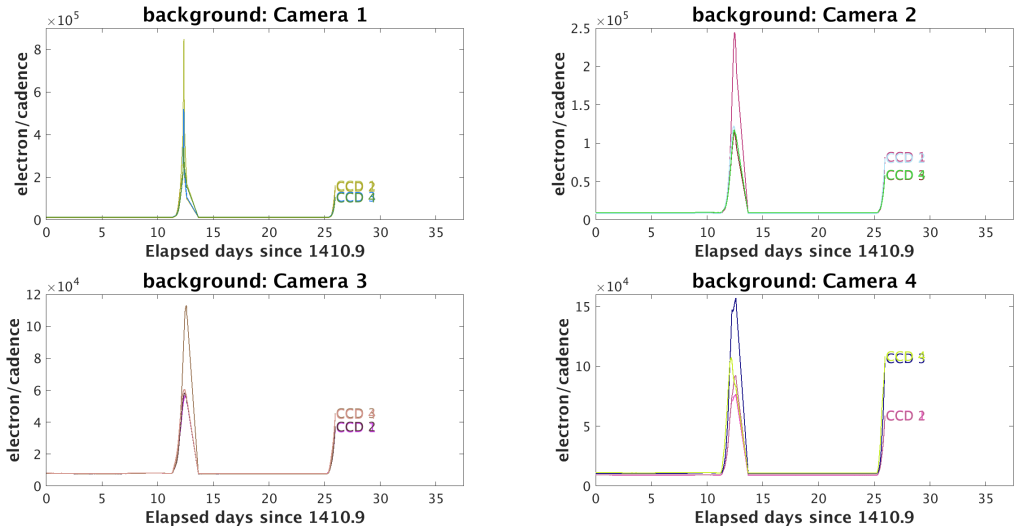


Figure 2: Median background flux across all targets on a given CCD in each camera. The changes are caused by variations in the orientation and distance of the Earth and Moon. The upturn at the end of each orbit is caused by the Earth rising above the sunshade.

## 1.4 Scattered Light

Figure 2 shows the median value of the background estimate for all targets on a given CCD as a function of time. Figure 3 shows the angle between each camera's boresight and the Earth or Moon—this figure can be used to identify periods affected by scattered light and the relative contributions of the Earth and Moon to the image backgrounds. In Sector 4,the main stray light feature are caused by the Earth rising above the sunshade at the end of each orbit. The Earth reaches a minimum of 35 degrees from the center of Camera 1, and strong glints appear between TJD 1422.2297 and 1423.5020 (orbit 15) and between TJD 1436.1047 and 1436.8353 (orbit 16).

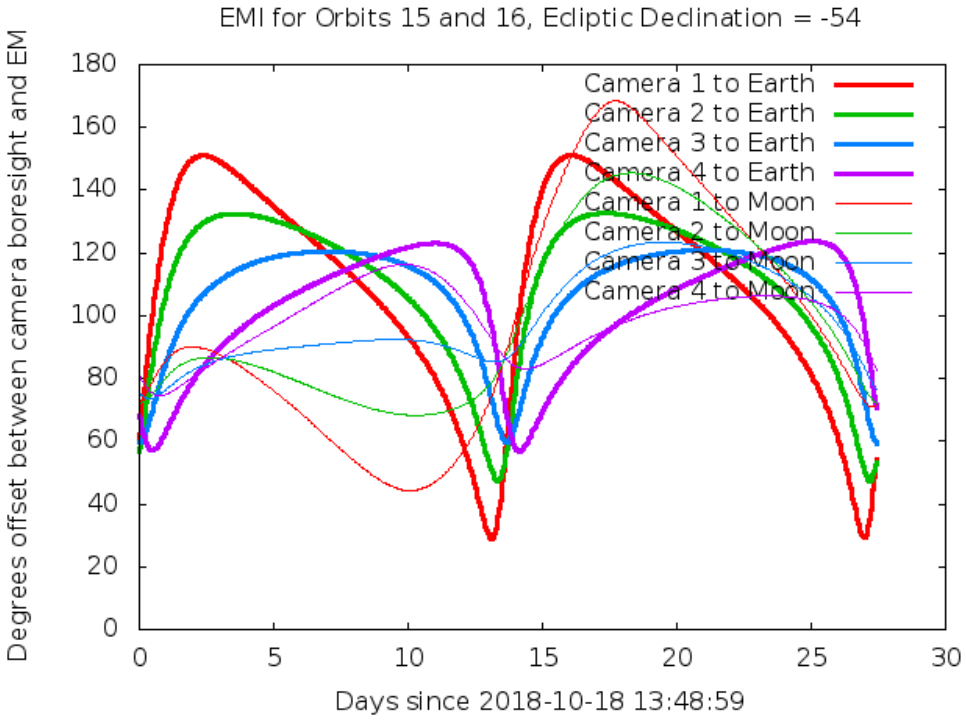


Figure 3: Angle between the four camera boresights and the Earth/Moon as a function of time. When the Earth/Moon moves within 37° of a camera's boresight, scattered light patterns and complicated features such as glints may appear. At larger angles, low level patchy features may appear. This figure can be used to identify periods affected by scattered light and the relative contributions of the Earth and Moon to the background. However, the background intensity and locations of scattered light features depend on additional factors, such as the Earth/Moon azimuth and distance from the spacecraft.

# 2 Data Anomaly Flags

See the SDPDD (§9) for a list of data quality flags and the associated binary values used for TESS data, and the instrument handbook for a more detailed description of each flag.

The following flags were not used in Sector 4: bits 2, 7, 9, 11, and 12 (Safe Mode, Cosmic Ray in Aperture, Discontinuity, Cosmic Ray in Collateral Pixel, and Straylight).

Cadence 133779 was marked with bit 1 (Attitude Tweak), based on the time that the guidestar table was replaced and observations resumed.

Cadences marked with bits 3, 4, and 6 (Coarse Point, Earth Point, and Reaction Wheel Desaturation Event) were marked based on spacecraft telemetry.

Cadences marked with bit 5 and 10 (Argabrightening Events and Impulsive Outlier) were identified by SPOC pipeline results. Bit 5 marks a sudden change in the background measurements. Bit 10 marks an outlier identified by PDC and omitted from the cotrending procedure.

Cadences marked with bit 8 (Manual Exclude) are ignored by PDC, TPS, and DV for cotrending and transit searches. In Sector 4, these cadences were identified using spacecraft

telemetry from the fine pointing system. All cadences with pointing excursions $>21$ arcseconds ($\sim$1 pixel) were flagged for manual exclude. See Figure 4 for an assessment of the performance of the detrending based on the final set of manual excludes.

FFIs were only marked with bit 6 (Reaction Wheel Desaturation Events). Only one or two FFIs are affected by each momentum dump.

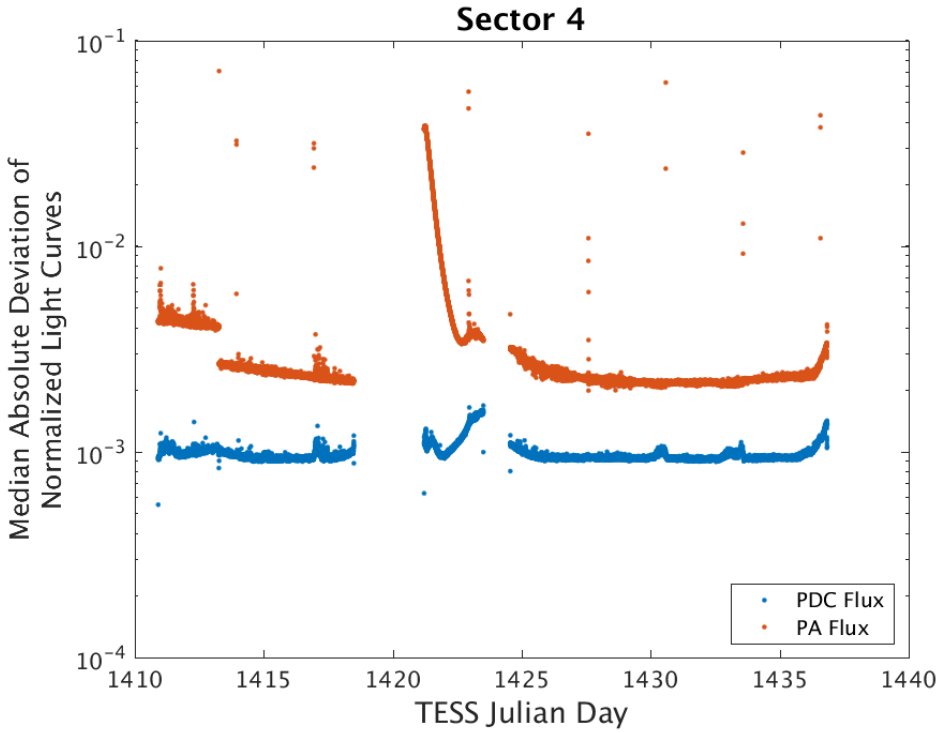


Figure 4: Median absolute deviation (MAD) for the 2-minute cadence data from Sector 4, showing the performance of the cotrending after identifying Manual Exclude data quality flags. The MAD is calculated in each cadence across stars with flux variations less than 1% for both the PA (red) and PDC (blue) light curves, where each light curve is normalized by its median flux value. The scatter in the PA light curves is much higher than that for the PDC light curves, and the outliers in the PA light curves are largely absent from the PDC light curves due to the use of the anomaly flags. Note that the first and last cadences in each orbit are treated as gaps by PDC.

# 3 Anomalous Effects

## 3.1 Thermal Effects

Heaters were turned on after the instrument anomaly, increasing the camera temperature by $\sim 20^{\circ}$ to approximately $-67^{\circ}$ C. Once the camera power was restored, the heaters were turned off and the camera temperatures returned to nominal within three days. The temperature increase caused changes in the camera focal plane scale and mean black levels of individual

CCD channels. The mean black levels are calibrated out in the SPOC pipeline. Changes in in focal plane cause changes in the raw photometry, but the PDC detrending alogorithm removes this effect for most targets.

## 3.2 Smear Correction Issues

1. Camera 2, CCD 1, Column 325: There is excess charge in the virtual smear region centered on Column 459, Row 2062. The source of this effect is unclear, but the charge causes a slight over-correction of the smear in this and adjacent columns.

2. Camera 4, CCD 4, Column 1794: There is a bright star in the upper buffer rows that bleeds into the upper serial register and effects the smear rows and corresponding smear correction in this column.

## 3.3 Black Flutter

Flutter in the mean black level was observed in Camera 1, CCD 2, cadences 142600 to 142790 and Camera 4, CCD 2, cadences 142510 to 142580. Similar oscilliations can be observed at the end of orbit 15 after the instrument anomaly (in addition to the long-term trend driven by temperature changes). See the instrument handbook for more details about overclock flutter.

## 3.4 Fireflies and Fireworks

Table 2 lists all firefly and fireworks events for Sector 4. These phenomena are small, spatially extended, comet-like features in the images that may appear one or two at a time (fireflies) or in large groups (fireworks). See the instrument handbook for a complete description.

Table 2: Sector Fireflies and Fireworks

| FFI Start | FFI End | Cameras | Description |
|---|---|---|---|
| 2018293202940 | 2018293205940 | 2, 3 | single firefly |
| 2018303135940 | 2018303142940 | 1 | single firefly |
| 2018306015940 | 2018306022940 | 1, 2 | single firefly |
| 2018308055940 | 2018308062940 | 1, 2 | fireflies |
| 2018308122940 | 2018308125940 | 2 | single firefly |
| 2018309015940 | 2018309022940 | 2 | single firefly |
| 2018309225940 | 2018309232940 | 3, 4 | single firefly |
| 2018312035940 | 2018312042940 | 1, 2 | fireflies |
| 2018317142940 | 2018317145940 | 2, 3, 4 | fireworks |

## 3.5 Timing Precision and Accuracy

The spacecraft clock slowly drifts relative to UTC time at a rate of a few 10s of milliseconds per day. The spacecraft clock kernel is used to correct this difference based on the measured

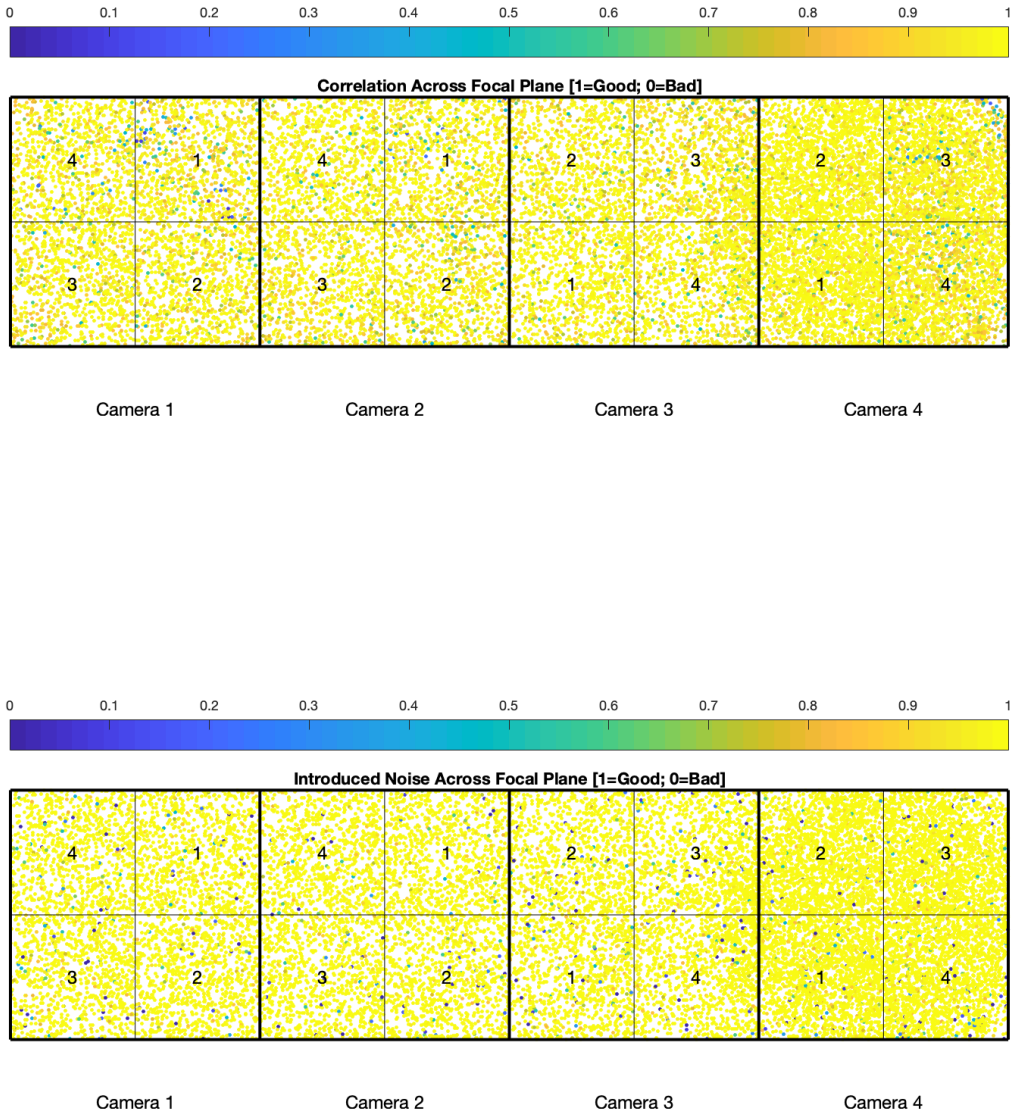


Figure 5: PDC residual correlation goodness metric (top panel) and PDC introduced noise goodness metric (bottom panel). The metric values are shown on a focal plane map indicating the camera and CCD location of each target. The correlation goodness metric is calibrated such that a value of 0.8 means there is less than 10% mean absolute correlation between the target under study and all other targets on the CCD. The introduced noise metric is calibrated such that a value of 0.8 means the power in broad-band introduced noise is only slightly above the level of uncertainties in the flux values.

drift rate. However, the clock kernel used to process Sector 4 data has a slight error in this measurement, resulting from extrapolation of timing measurements made during Sector

1. The reported TJD values in all data products are therefore offset by ∼1.6 seconds at the end of orbit 16 (2018-11-14 UTC). This error also implies that the durations of the individual cadences are underestimated by about 20 microseconds and the durations of FFIs are underestimated by about 280 microseconds. This issue will be corrected if the data are reprocessed in a future data release.

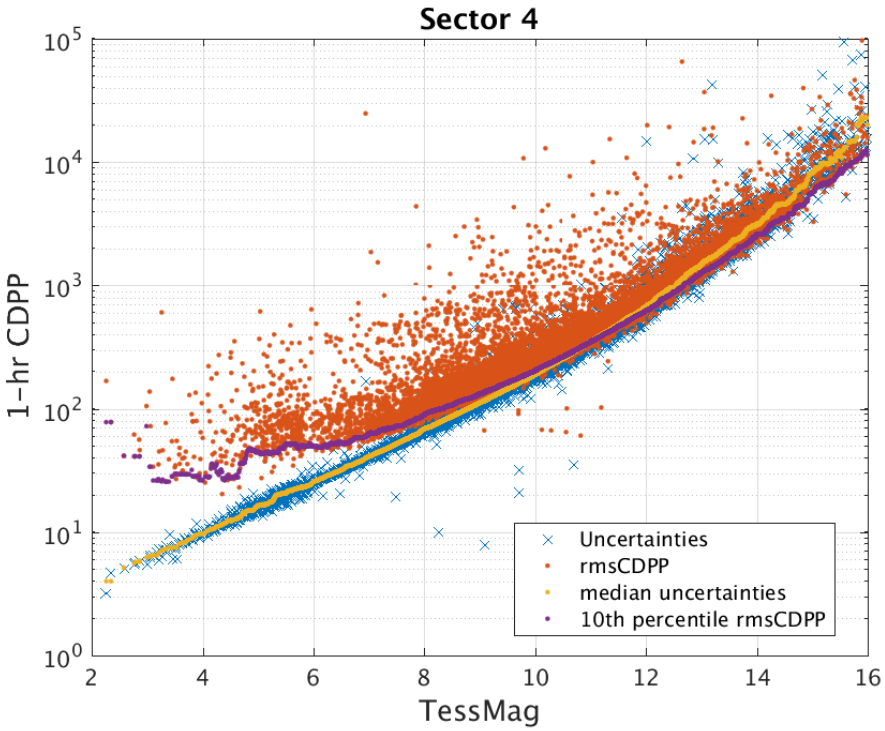


Figure 6: 1-hour CDPP. The red points are the RMS CDPP measurements for the 15997 light curves from Sector 4 plotted as a function of TESS magnitude. The blue x's are the uncertainties, scaled to 1-hour timescale. The purple curve is a moving 10th percentile of the RMS CDPP measurements, and the gold curve is a moving median of the 1-hr uncertainties.

# 4 Pipeline Performance and Results

## 4.1 Light Curves and Photometric Precision

Figure 5 gives the PDC goodness metrics for residual correlation and introduced noise on a scale between 0 (bad) and 1 (good). The performance of PDC is very good and generally uniform over the field of view.

Figure 6 shows the achieved Combined Differential Photometric Precision (CDPP) at 1-hour timescales for all targets.

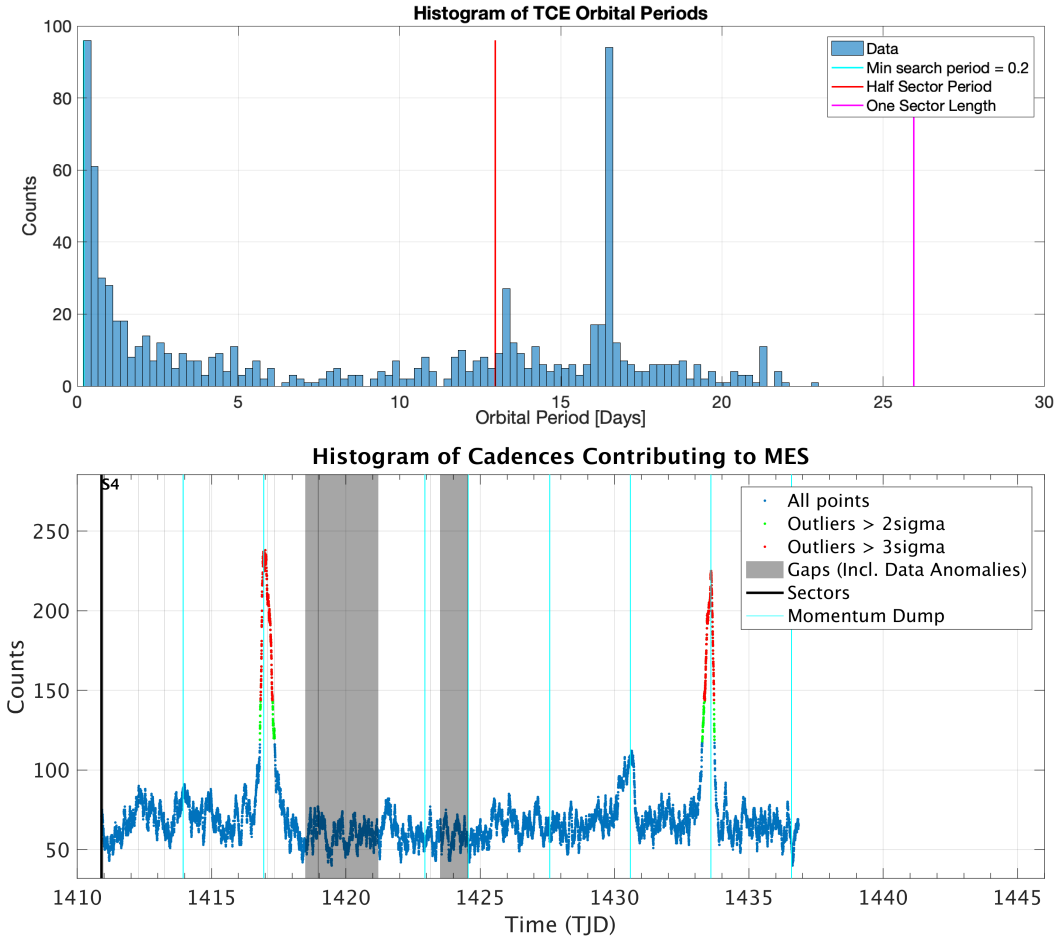


Figure 7: Top Panel: Histogram of orbital periods for 15997 TCEs identified by TPS in Sector 4. Bottom Panel: Number of TCEs at a given cadence exhibiting a transit signal. Isolated peaks are caused by a single event and result in spurious TCEs. Here, the peaks align with momentum dumps that are spaced at integer multiples of 2.5 days.

## 4.2 Transit Search and Data Validation

In Sector 4, the light curves of 15997 targets were subjected to the transit search in TPS. Of these, Threshold Crossing Events (TCEs) at the $7.1\sigma$ level were generated for 850 targets. Cadences at the end of each orbit, from 140238 to 141154 (orbit 15) and 150228 to 150754 (orbit 16) were excluded from the transiting planet search, due to the effects of rapidly changing scattered light features at these times (see Figure 2),

The top panel of Figure 7 shows the distribution of orbital periods for the TPS TCEs found in Sector 2. Narrow peaks in the histogram occur at approximately 14 and 16.5 days. These periods orrespond to spacings between momentum dumps in the first and second orbits, as shown in the bottom panel of Figure 7.

A search for additional TCEs in potential multiple planet systems was conducted in DV through calls to TPS. A total of 1167 TCEs were ultimately identified in the SPOC pipeline on 850 unique target stars. Table 3 provides a breakdown of the number of TCEs by target.

Note that targets with large numbers of TCEs are likely to include false positives.

Table 3: Sector 4 TCE Numbers

| Number of TCEs | Number of Targets | Total TCEs |
|---|---|---|
| 1 | 598 | 598 |
| 2 | 202 | 404 |
| 3 | 38 | 114 |
| 4 | 9 | 36 |
| 5 | 3 | 15 |
| – | 850 | 1167 |

Figure 8 shows the distribution of transit depths derived from limb-darkened transiting planet model fits for TCEs with SNR $> 7.1\,\sigma$. The model transit depths range down to the order of 100 ppm, but the bulk of the transit depths are considerably larger.

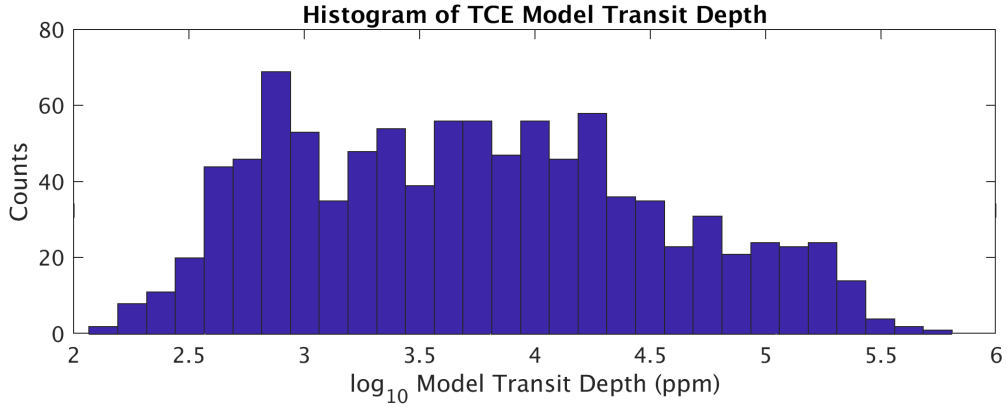


Figure 8: Histogram of limb-darkened transiting planet model transit depth for 986 TCEs with SNR $> 7.1\,\sigma$. Transit depth is displayed on a logarithmic scale in units of ppm.

# References


Jenkins, J. M. 2017, Kepler Data Processing Handbook: Overview of the Science Operations Center, Tech. rep., NASA Ames Research Center

Jenkins, J. M., Twicken, J. D., McCauliff, S., et al. 2016, in Proc. SPIE, Vol. 9913, Software and Cyberinfrastructure for Astronomy IV, 99133E

Li, J., Tenenbaum, P., Twicken, J. D., et al. 2019, *PASP*, 131, 024506

Twicken, J. D., Catanzarite, J. H., Clarke, B. D., et al. 2018, *PASP*, 130, 064502

Vanderspek, R., Doty, J., Fausnaugh, M., et al. 2018, TESS Instrument Handbook, Tech. rep., Kavli Institute for Astrophysics and Space Science, Massachusetts Institute of Technology

# Acronyms and Abbreviation List

**BTJD** Barycentric-corrected TESS Julian Date

**CAL** Calibration Pipeline Module

**CBV** Cotrending Basis Vector

**CCD** Charge Coupled Device

**CDPP** Combined Differential Photometric Precision

**COA** Compute Optimal Aperture Pipeline Module

**CSCI** Computer Software Configuration Item

**CTE** Charge Transfer Efficiency

**Dec** Declination

**DR** Data Release

**DV** Data Validation Pipeline Module

**DVA** Differential Velocity Aberration

**FFI** Full Frame Image

**FIN** FFI Index Number

**FITS** Flexible Image Transport System

**FOV** Field of View

**FPG** Focal Plane Geometry model

**KDPH** Kepler Data Processing Handbook

**KIH** Kepler Instrument Handbook

**KOI** Kepler Object of Interest

**MAD** Median Absolute Deviation

**MAP** Maximum A Posteriori

**MAST** Mikulski Archive for Space Telescopes

**MES** Multiple Event Statistic

**NAS** NASA Advanced Supercomputing Division

**PA** Photometric Analysis Pipeline Module

**PDC** Pre-Search Data Conditioning Pipeline Module

**PDC-MAP** Pre-Search Data Conditioning Maximum A Posteriori algorithm

**PDC-msMAP** Pre-Search Data Conditioning Multiscale Maximum A Posteriori algorithm

**PDF** Portable Document Format

**POC** Payload Operations Center

**POU** Propagation of Uncertainties

**ppm** Parts-per-million

**PRF** Pixel Response Function

**RA** Right Ascension

**RMS** Root Mean Square

**SAP** Simple Aperture Photometry

**SDPDD** Science Data Product Description Document

**SNR** Signal-to-Noise Ratio

**SPOC** Science Processing Operations Center

**SVD** Singular Value Decomposition

**TCE** Threshold Crossing Event

**TESS** Transiting Exoplanet Survey Satellite

**TIC** TESS Input Catalog

**TIH** TESS Instrument Handbook

**TJD** TESS Julian Date

**TOI** TESS Object of Interest

**TPS** Transiting Planet Search Pipeline Module

**UTC** Coordinated Universal Time

**XML** Extensible Markup Language